

RAPiD: Real-time Deterministic Trajectory Planning via Diffusion Behavior Priors for Safe and Efficient Autonomous Driving

Ruturaj Reddy^{1,2}, Hrishav Bakul Barua^{1,3}, Junn Yong Loo¹, Thanh Thi Nguyen²
and **Ganesh Krishnasamy¹**

¹School of Information Technology, Monash University, Malaysia

²Faculty of Information Technology, Monash University, Australia

³TCS Research, India

{rutaraj.reddy, hrishav.barua, loo.junnyong, thanh.nguyen9, ganesh.krishnasamy}@monash.edu

Abstract

Diffusion-based trajectory planners have demonstrated strong capability for modeling the multi-modal nature of human driving behavior, but their reliance on iterative stochastic sampling poses critical challenges for real-time, safety-critical deployment. In this work, we present RAPiD, a deterministic policy extraction framework that distills a pretrained diffusion-based planner into an efficient policy while eliminating diffusion sampling. Using score-regularized policy optimization, we leverage the score function of a pre-trained diffusion planner as a behavior prior to regularize policy learning. To promote safety and passenger comfort, the policy is optimized using a critic trained to imitate a predictive driver controller, providing dense, safety-focused supervision beyond conventional imitation learning. Evaluations demonstrate that RAPiD achieves competitive performance on closed-loop nuPlan scenarios with an 8 \times speedup over diffusion baselines, while achieving state-of-the-art generalization among learning-based planners on the interPlan benchmark. The official website of this work is: <https://github.com/ruturajreddy/RAPiD>

1 Introduction

In robotics, autonomy refers to a system’s capability to navigate environments independent of human control [Bekey, 2005]. Traditional planning methods rely on physics-based models, such as the kinematic bicycle model or Kalman filtering, and rule-based methods. While interpretable, these approaches rely on rigid rules and simplistic assumptions that struggle to adapt to complex, long-tail traffic scenarios [Treiber *et al.*, 2000]. Hence, the field has shifted towards learning-based methods [Scheel *et al.*, 2022; Rhinehart *et al.*, 2018], utilizing large-scale datasets such as nuPlan [Karnchanachari *et al.*, 2024] to mimic human driving. Despite its dominance, Imitation Learning (IL) struggles with multi-modal distributions, leading to the averaging of disparate behaviors (“model collapse”) [Codevilla *et al.*, 2018; Wang *et al.*, 2023]. This often yields unsafe, interpolated trajectories

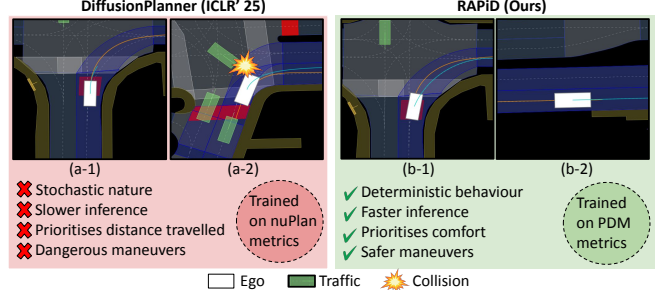


Figure 1: Figures (a-1) and (a-2) illustrate the limitations of the baseline DiffusionPlanner. Its computationally intensive, stochastic sampling (100ms latency) causes a delayed reaction, resulting in a collision. In contrast, Figures (b-1) and (b-2) demonstrate our proposed RAPiD framework. By distilling the diffusion prior into a deterministic policy trained on PDM safety metrics rather than nuPlan metrics, RAPiD achieves 8 \times faster inference. This efficiency enables timely decisions, resulting in a smooth, collision-free maneuver.

that compromise vehicle safety [Chen *et al.*, 2024; Shafiullah *et al.*, 2022]. To improve upon pure imitation, Offline Reinforcement Learning (Offline RL) was introduced to optimize a policy against a reward function while remaining within the support of the training data [Fujimoto *et al.*, 2019; Kumar *et al.*, 2019]. A central challenge in Offline RL is behavior regularization, which ensures the learned policy remains within the safe boundaries of the training data distribution. Traditional offline RL via weighted regression [Peng *et al.*, 2019; Kostrikov *et al.*, 2021] often suffers from “mode-covering,” where policies select out-of-distribution actions between behavioral modes [Chen *et al.*, 2024; Wang *et al.*, 2023].

Recently, diffusion models [Ho *et al.*, 2020; Song *et al.*, 2021] have emerged as state-of-the-art (SOTA) approaches for modeling complex, multi-modal distributions of human driving behavior. The SOTA method, such as DiffusionPlanner [Zheng *et al.*, 2025], uses a conditional diffusion model to jointly predict the ego-vehicle trajectory and neighboring vehicle trajectories, demonstrating robust performance without relying on rule-based guidance. Despite their robust performance, the deployment of diffusion models in safety-critical, real-time applications presents significant challenges of inference latency. The iterative process denoising process inherent to diffusion models requires tens to hundreds of sam-

pling steps to generate a single trajectory [Wang *et al.*, 2023; Ho *et al.*, 2020]. In autonomous driving, where making decisions and planning trajectories must be made within split second, diffusion models and their computational costs make it infeasible for real world usage. Furthermore, the stochastic nature of diffusion models can lead to inconsistent trajectories and decisions compromising safety making them highly unreliable [Wang *et al.*, 2023].

In this work, we propose RAPiD, where we distill the generative capabilities of diffusion models into a computationally efficient deterministic policy. We use Score Regularised Policy Optimization (SRPO) [Chen *et al.*, 2024], a novel algorithm that leverages a pre-trained diffusion model to regularize the policy gradient. Unlike methods requiring costly sampling, SRPO leverages the diffusion score function to estimate behavior density gradients directly. This enables the extraction of an efficient deterministic policy that balances reward maximization with behavioral fidelity. Since Offline RL relies heavily on reward signals, maximizing standard nuPlan metrics [Karnchanachari *et al.*, 2024] can yield high scores without guaranteeing closed-loop safety [Dauner *et al.*, 2023]. To ensure rewards correspond to genuinely safer trajectories rather than just numerical maximization, we train our critic using the Predictive Driver Model (PDM) [Dauner *et al.*, 2023; Yang *et al.*, 2024]. Our approach RAPiD is evaluated on the nuPlan [Karnchanachari *et al.*, 2024] benchmark. Using DiffusionPlanner [Zheng *et al.*, 2025] as the behavior prior and the PDM-based critic for policy extraction, we demonstrate that RAPiD can generate safer and reliable trajectories. As shown in Figure 1, our deterministic policy enables faster decision-making, allowing it to react in time to prevent collisions where the baseline fails. Experiments show that this approach surpasses the DiffusionPlanner [Zheng *et al.*, 2025] baseline in non-reactive closed-loop evaluation splits (*i.e.*, val14, test14, and test14-hard) [Karnchanachari *et al.*, 2024], while maintaining an 8× faster inference speedup. We also address the performance gap in reactive scenario and discuss challenges in transferring knowledge from generative frameworks to deterministic policies.

Our contributions are as follows:

- We present the first application of Score Regularised Policy Optimization [Chen *et al.*, 2024] to trajectory planning in autonomous driving, distilling a SOTA diffusion based planner [Zheng *et al.*, 2025] into a deterministic policy achieving **over 8× inference speedup** while maintaining performance.
- We demonstrate that score-based gradient regularization successfully bridges the expressivity of diffusion models with the **computational efficiency of deterministic policies**, enabling real-time trajectory planning in safety-critical autonomous driving environments.
- We validate our approach on nuPlan [Karnchanachari *et al.*, 2024] using **safety-focused PDM-based evaluation**, showing competitive performance on non-reactive scenarios without diffusion sampling overhead. We analyze the performance gap in reactive scenarios and discuss challenges in distilling knowledge from a generative model to a deterministic policy.

2 Related Work

2.1 Traditional and Learning-Based Planning

Traditional rule-based planners provide interpretability but lack adaptability, motivating Imitation Learning (IL), which unfortunately struggles with multi-modal mode averaging [Karnchanachari *et al.*, 2024; Chi *et al.*, 2025]. To address this, DiffusionPlanner [Zheng *et al.*, 2025] utilizes a transformer-based diffusion architecture for joint prediction and planning, while DiffusionES [Yang *et al.*, 2024] combines diffusion with evolutionary search to optimize black-box rewards. However, these methods suffer from high latency due to iterative denoising and stochastic sampling, rendering them computationally expensive for real-time safety-critical systems [Chen *et al.*, 2024; Wang *et al.*, 2023].

Recent works have increasingly adopted diffusion models [Sohl-Dickstein *et al.*, 2015; Ho *et al.*, 2020; Song *et al.*, 2021] for trajectory planning due to their ability to model complex, multi-modal distributions [Chi *et al.*, 2025; Ajay *et al.*, 2023]. In autonomous driving, DiffusionPlanner [Zheng *et al.*, 2025] employs a transformer-based diffusion architecture to jointly perform prediction and planning, effectively handling multi-modal interactions without rule-based refinement, while DiffusionES [Yang *et al.*, 2024] integrates diffusion modeling with evolutionary search to optimise trajectories using black-box reward functions. Despite achieving state-of-the-art performance, diffusion-based planners face major deployment challenges. Their iterative denoising process incurs substantial inference latency [Chen *et al.*, 2024], which is incompatible with the real-time decision-making demands of autonomous driving. Moreover, the stochastic nature of diffusion policies necessitates sampling many trajectories in parallel, often dozens, followed by post hoc selection [Wang *et al.*, 2023], resulting in high computational cost and limiting their suitability for safety-critical systems that require fast and deterministic behavior.

2.2 Policy Distillation and Efficiency

To improve efficiency, Offline RL explores extracting deterministic policies. While methods like Diffusion-QL [Wang *et al.*, 2023] and IDQL [Hansen-Estruch *et al.*, 2023] employ diffusion for value estimation, they still incur high inference costs from sampling. In contrast, SRPO [Chen *et al.*, 2024] avoids this by using the score function of a frozen behavior model to regularize the policy gradient directly. This allows the extraction of a deterministic policy that captures diverse behaviors without iterative sampling, achieving 8× speedup.

2.3 Safety-Guided Evaluation and PDM Metrics

Trajectory planner evaluation has traditionally relied on open-loop displacement errors (*e.g.*, L_2 distance) or standard closed-loop simulation scores from benchmarks such as nuPlan [Karnchanachari *et al.*, 2024]. However, Dauner *et al.* [Dauner *et al.*, 2023] identified a “fundamental misalignment” between open-loop metrics and closed-loop driving reliability, showing that strong open-loop performance does not correlate with collision-free behavior, and that rule-based baselines such as PDM [Dauner *et al.*, 2023] often outperform learning-based methods in closed-loop settings

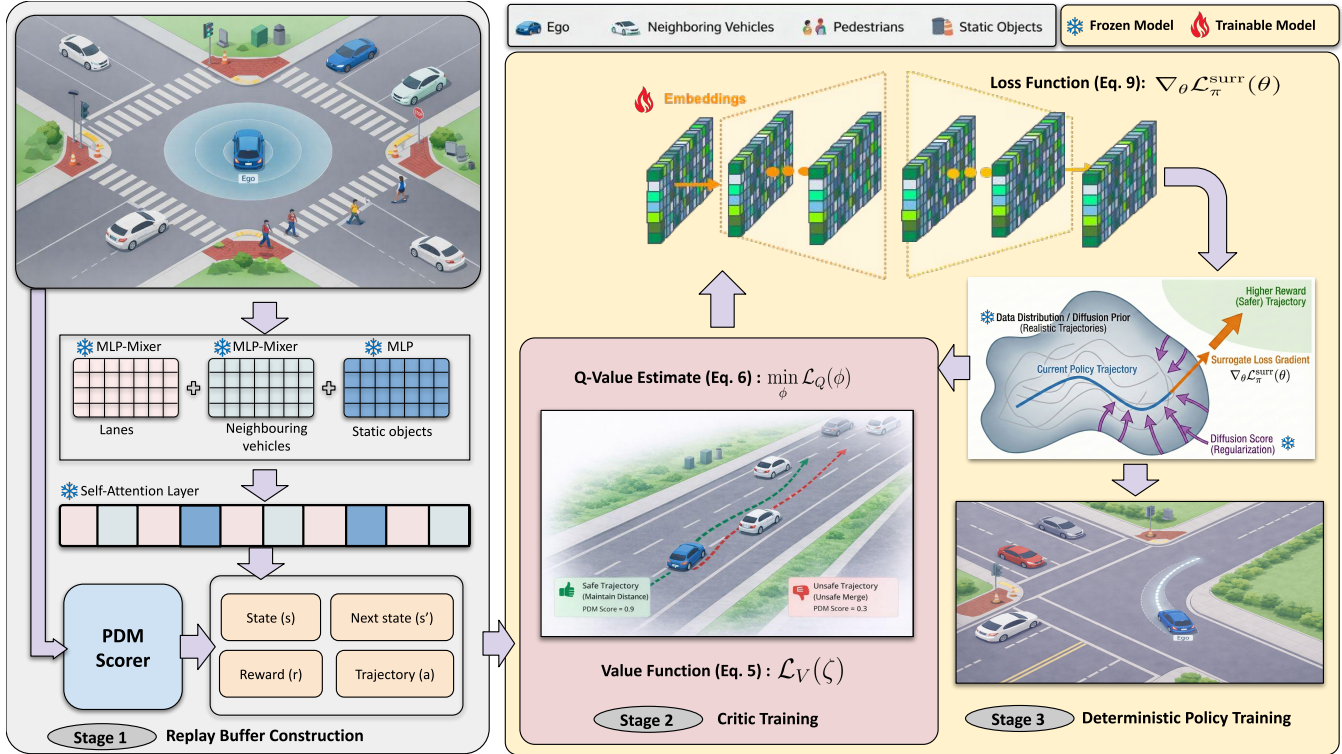


Figure 2: **Overview of the proposed framework** (Section 3.5). Stage 1 involves offline replay buffer construction, where raw sensor data is processed by a frozen DiffusionPlanner encoder to generate rich latent state embeddings (s). Ground truth trajectories are evaluated by the PDM Scorer to assign rewards (r) based on safety and comfort metrics, creating a scored dataset. Stage 2 focuses on Critic Training via Implicit Q-Learning. The critic learns to estimate the Q-value $\mathcal{L}_Q(\phi)$ by evaluating ground truth trajectories (a) conditioned on the frozen embeddings (s), effectively distinguishing between safe (high PDM score) and unsafe behaviors. Stage 3 performs Deterministic Policy Training. A Transformer-based policy is distilled using the surrogate loss gradient $\nabla_\theta \mathcal{L}_\pi^{\text{surr}}(\theta)$. This gradient fuses the Critic’s guidance (maximizing safety rewards) with the Frozen Diffusion Prior’s score function to regularize the policy toward realistic manifolds, enabling fast, one-step deterministic inference.

by strictly enforcing safety constraints. Consequently, recent works [Yang *et al.*, 2024] have shifted toward closed-loop evaluation that prioritizes collision avoidance, drivable area compliance, and progress as primary objectives. Following this paradigm, we evaluate our policy on the nuPlan closed-loop benchmark using PDM metrics [Yang *et al.*, 2024], rather than open-loop displacement errors, to ensure robustness in real-world driving scenarios.

3 Methodology

3.1 Problem Formulation

The trajectory planning task generates safe and efficient future trajectories for an ego vehicle (*e.g.*, self-driving car) in a dynamic environment. At time step t , the system observes historical states (t_h) of the ego and surrounding environment. Following the nuPlan benchmark [Karnchanachari *et al.*, 2024], the model processes spatial map data \mathcal{S} (*e.g.*, lane geometry, traffic lights, speed limits) and temporal agent data \mathcal{T} (*i.e.*, positions, velocities, headings) to predict the vehicle’s trajectory over the next future time (t_f) steps, represented as $\mathcal{Y} = \{\hat{X}_{t+1:t+t_f}\}$. The objective is to generate trajectories that adhere to traffic rules while making progress.

3.2 Pretrained Diffusion Planner

We utilize a pretrained DiffusionPlanner [Zheng *et al.*, 2025] for modeling multi-modal human driving behavior. DiffusionPlanner is built upon the diffusion transformer (DiT) architecture [Peebles and Xie, 2023] and jointly models both prediction and planning tasks within the same architecture [Zheng *et al.*, 2025], enabling cooperative behaviors between vehicles. The forward diffusion process gradually adds Gaussian noise to trajectories $x^{(0)}$ over continuous time $t \in [0, 1]$ [Ho *et al.*, 2020; Song *et al.*, 2021]:

$$q_{t|0}(x^{(t)}|x^{(0)}) = \mathcal{N}(x^{(t)}|\alpha_t x^{(0)}, \sigma_t^2 I), \quad (1)$$

where α_t and σ_t are the noise schedule parameters. The model learns to recover the data distribution from noisy data by training a network $\mu_\theta(x^{(t)}, t, C)$ to predict the original trajectory given noised data and conditions C . This process learns the gradient of the trajectory score function [Song *et al.*, 2021; Zheng *et al.*, 2025], allowing the model to capture complex multi-modal distributions in human planning data. While DiffusionPlanner achieves SOTA closed-loop performance, the iterative denoising process which often requires tens to hundreds of diffusion steps during inference, presents

a significant computational bottleneck for real-time applications [Wang *et al.*, 2023; Chen *et al.*, 2024].

3.3 Score Regularized Policy Optimization

To overcome the slow sampling speed of diffusion models, we employ Score Regularized Policy Optimization (SRPO) [Chen *et al.*, 2024] to extract an efficient deterministic inference policy π_θ . SRPO formulates policy learning using a reverse-KL objective that is inherently mode-seeking:

$$\begin{aligned} \max_{\theta} \mathcal{L}_\pi(\theta) &= \mathbb{E}_{s \sim \mathcal{D}_\mu, a \sim \pi_\theta} [Q_\phi(s, a)] \\ &\quad - \frac{1}{\beta} D_{KL}[\pi_\theta(\cdot|s) || \mu(\cdot|s)], \end{aligned} \quad (2)$$

where $Q_\phi(s, a)$ is a learned Q-value function, $\mu(\cdot|s)$ represents the behavior distribution, and β is a temperature coefficient. This contrasts with weighted regression methods that suffer from mode-covering issues [Chen *et al.*, 2024; Wang *et al.*, 2023]. The key insight of SRPO is to regularize the policy gradient directly using the behavior distribution's score function. By decomposing the KL term and applying the reparameterization trick, the gradient becomes:

$$\begin{aligned} \nabla_\theta \mathcal{L}_\pi(\theta) &= \mathbb{E}_{s \sim \mathcal{D}_\mu} \left[\left(\nabla_a Q_\phi(s, a) \Big|_{a=\pi_\theta(s)} \right. \right. \\ &\quad \left. \left. + \frac{1}{\beta} \underbrace{\nabla_a \log \mu(a|s) \Big|_{a=\pi_\theta(s)}}_{\approx -\epsilon^*(a_t|s, t) / \sigma_t} \right) \nabla_\theta \pi_\theta(s) \right]. \end{aligned} \quad (3)$$

The behavior distribution's score function $\nabla_a \log \mu(a|s)$ here can be effectively approximated by the pretrained diffusion behavior model [Chen *et al.*, 2024; Song *et al.*, 2021]:

$$\nabla_a \log \mu(a|s) \approx -\frac{\epsilon_\psi(a_t|s, t)}{\sigma_t} \Big|_{t \rightarrow 0}, \quad (4)$$

where $\epsilon_\psi(a_t|s, t)$ is the noise prediction model of Diffusion-Planner. This enables us to use the powerful generative capabilities of diffusion modeling while skipping the computationally intensive and time-consuming diffusion sampling scheme, both during training and evaluation. To the best of our knowledge, this work is the first to apply the SRPO method in the field of trajectory planning problem. For Q-networks, we use implicit Q-learning (IQL) [Kostrikov *et al.*, 2021] to decouple critic training from actor training [Chen *et al.*, 2024]. The core method is expectile regression, which down-weights suboptimal trajectories with lower Q-values, removing the need of an explicit policy [Kostrikov *et al.*, 2021; Chen *et al.*, 2024].

3.4 Safety-Aware Reward Design via PDM Scorer

To ensure that the learned policy follows the safety requirements, we integrate the Predictive Driver Model (PDM) scorer as the reward function. The PDM scorer evaluates trajectories based on traffic rule compliance, time-to-collision (TTC), drivable area adherence, and passenger comfort [Dauner *et al.*, 2023]. Specifically, we employ the enhanced PDM scorer from Diffusion-ES [Yang *et al.*, 2024] which is based on the standard PDM metrics [Dauner *et al.*, 2023], but includes additional metrics that penalize proximity to the leading agent and enforce speed limits, enhancing safety of the trajectory as well as making it comfortable. For additional details on PDM scoring, please refer to Section S1 of *Supplementary Material*.

3.5 Proposed Method

Figure 2 showcases the overall pipeline of our method consisting of input encoding and trajectory prediction. This subsection outlines the structure of our method. Our training procedure follows a modified SRPO pipeline adapted for the nuPlan benchmark [Karnchanachari *et al.*, 2024]. The training process is divided into three stages, *i.e.*, offline replay buffer creation with PDM scored ground truth trajectories, critic training via implicit Q-learning, and policy extraction using score regularization. Please refer to pseudocode available in Section S2 of *Supplementary Material*.

Stage 1: Offline Replay Buffer Creation. An offline replay buffer $[s, s', a, r]$ consists of state (s), next state (s'), action or trajectory (a), and reward (r). The states and next states are rich state latent encodings of the raw input (history of surrounding dynamic as well as static actors) generated by utilising only the pretrained encoder layer of the Diffusion-Planner [Zheng *et al.*, 2025]. This accelerates the subsequent training stages by reducing the dimensionality and representing the complexity of the input space in a latent dimension. We utilize ground truth trajectories from the nuPlan dataset to make sure the critic and policy learn realistic expert demonstrations. Each trajectory is evaluated using the Predictive Driver Model (PDM) [Yang *et al.*, 2024] scorer to obtain a reward r based on safety and comfort metrics. This reward signal directs the policy to select safer and more comfortable trajectories.

Stage 2: Critic Training. The critic estimates the rewards of the trajectories in given encoded states without requiring explicit policy queries which is a characteristic of Implicit Q-Learning (IQL) [Chen *et al.*, 2024]. IQL employs expectile regression to learn a value function, $V_\zeta(s)$, which prioritizes high reward trajectories while reducing extrapolation to out-of-distribution regions. The value function is optimized using an asymmetric squared loss function:

$$\mathcal{L}_V(\zeta) = \mathbb{E}_{(s, a) \sim \mathcal{D}^\mu} [L_2^\tau(Q_\phi(s, a) - V_\zeta(s))], \quad (5)$$

where \mathcal{L}_2^τ represents the asymmetric squared loss with expectile $\tau \in (0.8, 1)$. A value of $\tau > 0$ down-weights suboptimal actions associated with lower Q-values, focusing learning on safer trajectories. Subsequently, the Q-function is optimized using the standard temporal difference error:

$$\mathcal{L}_Q(\phi) = \mathbb{E}_{(s, a, s') \sim \mathcal{D}^\mu} \left[\left\| r(s, a) + \gamma V_\zeta(s') - Q_\phi(s, a) \right\|_2^2 \right]. \quad (6)$$

Here, r corresponds to the trajectory based reward obtained from replay buffer, and γ represents the discount factor. By operating on the frozen embeddings e_s , the critic converges faster than end-to-end approaches that process raw sensor data. Concurrently, we pretrain a deterministic policy $\pi_{\theta_{init}}$ to learn high reward trajectories in the replay buffer using advantage-weighted regression:

$$\begin{aligned} \mathcal{L}_{\pi_{init}}(\theta) &= \mathbb{E}_{(e_s, a) \sim \mathcal{D}} \left[\exp \left(\beta_{AWR}(Q_\phi(e_s, a) - V_\zeta(e_s)) \right) \right. \\ &\quad \left. \cdot \|a - \pi_\theta(e_s)\|^2 \right]. \end{aligned} \quad (7)$$

This objective forces the policy to clone actions with high estimated rewards (advantages). This pretrained policy $\pi_{\theta_{init}}$ provides a stable initialization for the score regularized optimization in Stage 3 which accelerates convergence.

Stage 3: Policy Extraction via Score Regularization. A deterministic policy, π_θ , is extracted which maps the encoded state e_s to a trajectory. To ensure the policy remains within the support of valid driving behaviors, we use the pretrained DiffusionPlanner [Zheng *et al.*, 2025] as a frozen behavioral prior. The policy is trained to maximize the Q-value, subject to a constraint that aligns its behavior with the diffusion model’s score function:

$$\theta \leftarrow \theta + \lambda_\pi \nabla_\theta \mathcal{L}_\pi^{\text{surr}}(\theta), \quad (8)$$

with the surrogate gradient defined as:

$$\begin{aligned} \nabla_\theta \mathcal{L}_\pi^{\text{surr}}(\theta) &\approx \mathbb{E}_s \left[\nabla_a Q_\phi(s, a) |_{a=\pi_\theta(s)} \right. \\ &\quad \left. - \frac{1}{\beta} \mathbb{E}_{t, \epsilon} \omega(t) (\epsilon_\psi(a_t | s, t) - \epsilon) |_{a_t = \alpha_t \pi_\theta(s) + \sigma_t \epsilon} \right] \quad (9) \\ &\quad \nabla_\theta \pi_\theta(s). \end{aligned}$$

Here, the term $(\epsilon_\psi(a_t | e_s, t) - \epsilon)$ approximates the score function $\nabla_a \log \mu(a | e_s)$ of the diffusion prior. This term functions as a regularizer, guiding the policy towards realistic behaviors within high-density data regions, without the computational cost of iterative diffusion sampling during inference.

4 Experiments

4.1 Experiment Setup

RAPiD is implemented in PyTorch and trained using an A40 GPU (48GB VRAM) on Monash University’s M3 Cluster. We evaluate robustness and accuracy across two datasets: nuPlan [Karnchanachari *et al.*, 2024] and interPlan [Hallgarten *et al.*, 2024]. To assess performance, we employ three evaluation frameworks: nuPlan scores for planning quality, interPlan scores with breakdown analysis for scenario-specific performance, and PDM scorer metrics [Yang *et al.*, 2024] for safety and comfort assessment. SOTA methods used for comparison are listed in Tables 1 and 3.

4.2 Evaluation Results

nuPlan Benchmark Performance. We evaluate our method against SOTA baselines, including learning-based planners (PDM-Open [Dauner *et al.*, 2023], UrbanDriver [Scheel *et al.*, 2022], Gameformer [Huang *et al.*, 2023], PlanTF [Chi *et al.*, 2025], PLUTO [Cheng *et al.*, 2024], DiffusionPlanner [Zheng *et al.*, 2025]) and rule-based planners (IDM [Treiber *et al.*, 2000], PDM-Closed [Dauner *et al.*, 2023], PDM-Hybrid [Dauner *et al.*, 2023]). Table 1 summarizes performance on the nuPlan benchmark. By incorporating PDM-based scoring into critic training, our method demonstrates improvements in non-reactive (NR) planning. Our method achieves NR scores of 90.19 on val14, 89.98 on test14, and 76.09 on test14-hard, consistently outperforming the DiffusionPlanner baseline (89.87, 89.87, and 75.53 respectively). Table 2 shows our method is 8× faster than DiffusionPlanner and also surpasses PDM-Open and UrbanDriver in inference speed. While slightly slower than PlanTF and Pluto, our method outperforms both by an average of 4.2

points across all metrics. In the reactive (R) environment, our method achieves competitive performance (81.86 on test14 compared to 82.93 for the baseline). This marginal difference stems from two factors. First, our deterministic policy forgoes the multi-modal sampling capability of diffusion-based models, which enables exploration of diverse reactive behaviors during closed-loop evaluation. Second, our PDM-based training objective explicitly reweights safety and comfort metrics, increasing emphasis on comfort (2 to 5) and proximity (0 to 5) while reducing progress weight (5 to 2) compared to the nuPlan scorer. Consequently, our method prioritizes comfortable, safer trajectories over aggressive maneuvers that achieve higher progress scores in reactive scenarios. In lane following scenarios, our method maintains closer distance to the centerline (Figure 3(a-2)) with smoother acceleration patterns and reduced braking frequency when following lead vehicles (Figure 3(a-1)). During stopping scenarios, our approach maintains larger safety margins by reducing speed earlier (Figure 3(b-2)), whereas DiffusionPlanner exhibits shorter following distances (Figures 3(b-1)). For lane changes, our method executes gradual merges with lower yaw rates (Figures 3(c-2) compared to DiffusionPlanner’s sharper maneuvers (Figure 3(c-1)). At intersections, DiffusionPlanner often exhibits hesitation followed by abrupt maneuvers, leading to near-miss scenarios (Figure 3(d-1)) or actual collisions due to delayed decision-making (Figure 1(a-2)). In contrast, our method demonstrates decisive, timely planning, executing smooth and assertive turns with controlled acceleration (Figure 3(d-2)) that successfully avoid collisions where the baseline fails (Figure 1(b-1, b-2)). See Section S3.1 in *Supplementary Material* for a detailed frame-by-frame analysis. These behavioral differences reflect our PDM-based training objective, which prioritizes comfort and proximity distance over route progress, contrasting with nuPlan’s emphasis on progress metrics at the expense of passenger comfort.

interPlan Benchmark Analysis. We evaluate our approach against SOTA baselines, including learning-based planners (UrbanDriver [Scheel *et al.*, 2022], GC-PPG [Hallgarten *et al.*, 2023], Gameformer [Huang *et al.*, 2023], PDM-Open [Dauner *et al.*, 2023], DTPP [Huang *et al.*, 2024], DiffusionPlanner [Zheng *et al.*, 2025]) and rule-based planners (IDM [Treiber *et al.*, 2000], IDM+MOBIL [Kesting *et al.*, 2007], PDM-Closed [Dauner *et al.*, 2023]). The interPlan scorer extends standard nuPlan metrics (compliance, safety, comfort) with scenario-specific requirements. It measures lane change completion rates relative to goal requirements and applies multiplicative progress penalties for failures to pass obstacles like parked cars or construction zones. Scenarios receive zero scores for collisions, drivable area violations, extended stationarity, or getting stuck behind obstacles. Direction compliance penalties are disabled for overtaking and accident scenarios where oncoming lane usage is necessary. Table 3 presents results on the interPlan benchmark, which addresses a critical nuPlan limitation: achieving high scores through simple lane-following with minimal interaction. interPlan augments scenario goals to require multiple lane changes and initializes varying traffic densities by spawning agents around the ego vehicle at maximum spacings of 100m (low traffic density, LTD), 50m (medium traf-

Table 1: Closed-loop planning results on nuPlan benchmark. Bold values indicate best performance in each category. *: Methods using pre-computed reference paths benefit from additional prior information. **NR**: non-reactive evaluation. **R**: reactive evaluation.

Type	Methods	Val14		Test14-hard		Test14	
		NR	R	NR	R	NR	R
Expert	Log-replay	93.53	80.32	85.96	68.80	94.03	75.86
Rule-based & Hybrid	IDM [Treiber <i>et al.</i> , 2000]	75.60	77.33	56.15	62.26	70.39	74.42
	PDM-Closed [Dauner <i>et al.</i> , 2023]	92.84	92.12	65.08	75.19	90.05	91.63
	PDM-Hybrid [Dauner <i>et al.</i> , 2023]	92.77	92.11	65.99	76.07	90.10	91.28
	GameFormer [Huang <i>et al.</i> , 2023]	79.94	79.78	68.70	67.05	83.88	82.05
	PLUTO [Cheng <i>et al.</i> , 2024]	92.88	76.88	80.08	76.88	92.23	90.29
	Diffusion Planner w/ refine [Zheng <i>et al.</i> , 2025]	94.26	92.90	78.87	82.00	94.80	91.75
Learning-based	PDM-Open* [Dauner <i>et al.</i> , 2023]	53.53	54.24	33.51	35.83	52.81	57.23
	UrbanDriver [Scheel <i>et al.</i> , 2022]	68.57	64.11	50.40	49.95	51.83	67.15
	GameFormer w/o refine [Huang <i>et al.</i> , 2023]	13.32	8.69	7.08	6.69	11.36	9.31
	PlantTF [Chi <i>et al.</i> , 2025]	84.27	76.95	69.70	61.61	85.62	79.58
	PLUTO w/o refine* [Cheng <i>et al.</i> , 2024]	88.89	78.11	70.03	59.74	89.90	78.62
	DiffusionPlanner [Zheng <i>et al.</i> , 2025]	89.87	82.80	75.99	69.22	89.19	82.93
	RAPiD (Ours)	90.19	81.84	76.09	66.94	89.98	81.86

Table 3: **Quantitative results**. The interPlan benchmark scores. interPlan is aggregated scores, followed by specific scenario type scores. **Const.**: Construction, **Acc.**: Accident, **Jayw.**: Jaywalking Pedestrians, **Overt.**: Overtaking, **LTD**: Low Traffic Density, **MTD**: Medium Traffic Density, **HTD**: High Traffic Density.

Type	Method	interPlan	Const.	Acc.	Jayw.	Nudge	Overt.	LTD	MTD	HTD
Rule-based	IDM [Treiber <i>et al.</i> , 2000]	31	0	0	66	0	0	61	61	61
	IDM+MOBIL [Kesting <i>et al.</i> , 2007]	31	21	0	66	0	0	71	21	70
	PDM-Closed [Dauner <i>et al.</i> , 2023]	42	18	0	48	74	9	62	62	62
Learning-based	Urban Driver [Scheel <i>et al.</i> , 2022]	4	0	0	0	0	0	29	0	30
	GC-PGP [Hallgarten <i>et al.</i> , 2023]	10	0	0	0	0	0	18	16	44
	GameFormer [Huang <i>et al.</i> , 2023]	11	0	0	48	0	0	0	20	21
	PDM-Open [Dauner <i>et al.</i> , 2023]	25	13	0	56	36	8	29	29	26
	DTPP [Huang <i>et al.</i> , 2024]	25	18	18	44	10	0	40	36	34
	DiffusionPlanner [Zheng <i>et al.</i> , 2025]	25	9	0	26	60	25	40	21	16
	RAPiD (Ours)	27	11	0	28	62	26	42	27	23

fic density, MTD), and 33m (high traffic density, HTD). The benchmark comprises 80 scenarios across eight categories testing planner generalization to long-tail situations. Lateral maneuvering is evaluated through construction zones (Const., navigating around traffic cones), accident sites (Acc., maneuvering around crashed vehicles), jaywalking pedestrians (Jayw., handling unexpected crossings at bus stops), nudging (carefully passing parked vehicles within lane), and overtaking (safe passage through oncoming lanes). Please see Section S3.2 of *Supplementary Material* for details. Longitudinal interaction is tested through lane changes under LTD, MTD, and HTD conditions with varying traffic environments (conservative, assertive, mixed). Each category contains 10 instances. Unlike nuPlan, which can be solved primarily through lane-following, these scenarios explicitly require complex reasoning, proactive interaction, and robust generalization to uncommon situations. Our approach achieves the highest interPlan score among learning-based methods with an aggregate score of 27, outperforming PDM-Open and DiffusionPlanner. For lateral maneuvers, our method scores 62 in nudging scenarios (versus DiffusionPlanner’s 60) and 26 in overtaking—the highest among both learning-based and rule-based methods. For longitudinal interactions, performance improvements increase with traffic density: 42 versus 40 in LTD, 27 versus 21 in MTD, and 23 versus 16 in HTD.

These gains in denser conditions demonstrate our method’s ability to navigate between vehicles and complete required lane changes without freezing or causing safety violations. In MTD and HTD scenarios with reduced agent spacing (50m and 33m), our method shows improved gap selection and timing compared to DiffusionPlanner. While rule-based methods achieve highest performance on nuPlan, they fail to meet interPlan requirements in several scenarios. Our learning-based model demonstrates the adaptability required for interactive scenarios while maintaining competitive performance.

Predictive Model Safety and Comfort Analysis. Figure 4 provides a metric-level breakdown of PDM scores in the reactive environment across Val14, Test14, and Test14-hard splits. Both models are evaluated in the same reactive closed-loop setting but scored using the PDM metric rather than the standard nuPlan scorer. This analysis shows the improved safety-critical metrics while showcasing the reasoning behind the lower score on nuPlan benchmark for reactive environment.

Safety Metrics. Our method demonstrates improved collision avoidance performance across all splits. On Val14, the collision-avoidance rate increases from 94.67% to 95.50%, and on Test14-Hard from 91.99% to 93.10%. Both models maintain perfect drivable area compliance (100%) and high driving direction compliance (our method achieves 98.90%, 98.80%, and 96.90% across the three splits). Speed limit

Table 2: Inference time comparison across learning based methods.

Method	Time (ms)
PDM-Open [Dauner <i>et al.</i> , 2023]	14.67
UrbanDriver [Scheel <i>et al.</i> , 2022]	78.42
PlanTF [Chi <i>et al.</i> , 2025]	4.51
Pluto [Cheng <i>et al.</i> , 2024]	9.19
DiffusionPlanner [Zheng <i>et al.</i> , 2025]	100.91
RAPiD (Ours)	12.41

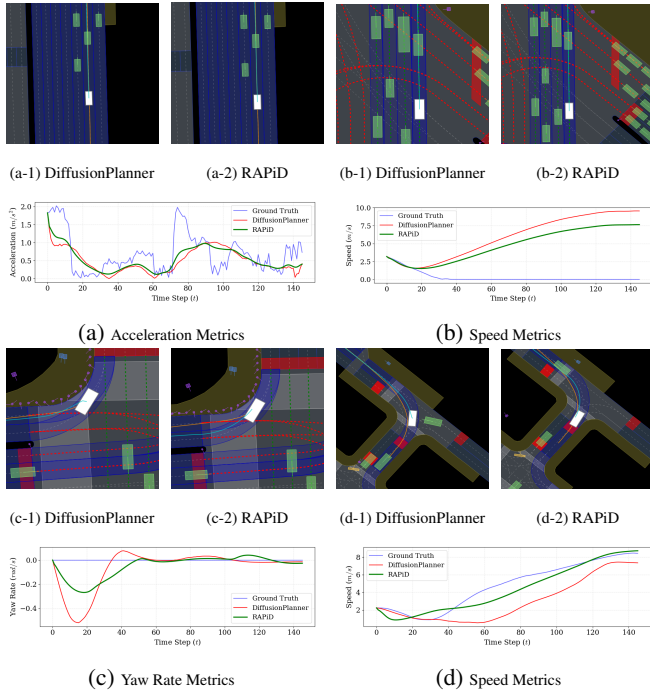


Figure 3: Qualitative results across four scenarios in nuPlan: (a) Following Lane, (b) Stopping with Lead, (c) Starting Right Turn, and (d) Low Speed Maneuvering. Each figure displays the generated trajectories for DiffusionPlanner and RAPiD (top) along with their corresponding Comfort metrics (bottom) including acceleration, speed, and yaw rate demonstrating the smoother control exerted by RAPiD compared to the baseline DiffusionPlanner.

compliance also improved on Test14-Hard as our method reaches 98.20% compared to the DiffusionPlanner’s 97.12%. These results validate that the critic successfully guides the policy toward safer trajectories.

Comfort Metrics. On Val14, our method achieves a comfort score of 0.9850 compared to 0.9787 for the DiffusionPlanner. On Test14, comfort increases from 0.9823 to 0.9890, while on Test14-Hard it improves from 0.9758 to 0.9800. Proximity scores show similar improvement, *i.e.*, 0.9800 versus 0.9694 (Val14), 0.9820 versus 0.9753 (Test14), and 0.9610 versus 0.9543 (Test14-Hard). As well as improvements in the lane-following performance across all splits directly reflect the PDM scorer’s penalties on jerk (comfort weight increased from 2 to 5) and vehicle in front distance (proximity weight introduced at 5). The results demonstrate that our method generates trajectories that are both smoother and safer with respect to neighboring agents in the nuPlan environment.

Progress Metrics. On Val14, progress decreases from 0.9374 to 0.8850; on Test14, from 0.9408 to 0.8920; and on Test14-Hard, from 0.8977 to 0.8850. This trade-off directly reflects the PDM scorer’s focus on safety, which reduces the progress metrics weight from 5 to 2 while increasing safety-critical weights. This behavior aligns with real-world situation, where passenger comfort and collision avoidance are more important over travel distances. The trade-off across all evaluation splits combined with improvements in TTC met-

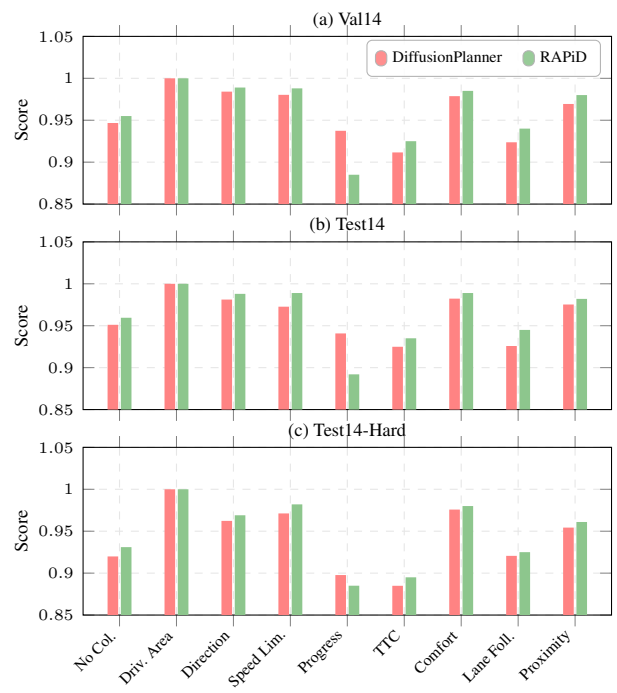


Figure 4: Breakdown of PDM scorer sub-metrics across (a) Val14, (b) Test14, and (c) Test14-Hard splits. RAPiD (Green) consistently outperforms DiffusionPlanner (Red) in critical safety metrics (*No Collision*, *TTC*) while trading *Progress* for safer maneuvers. **Metric Definitions:** **No Col.**: No Collision, **Driv. Area**: Drivable Area, **Speed Lim.**: Speed Limit, **TTC**: Time-to-Collision, **Lane Fall.**: Lane Following.

rics confirms that our method is making safety focused decisions rather than risky maneuvers for progressing distance resulting in lower scores in reactive environment. progressing distance resulting in lower scores in reactive environment progressing distance resulting in lower scores in reactive environment

5 Conclusion

This work addresses the computational inefficiency and stochastic behavior of diffusion-based trajectory planning through efficient policy distillation. By extracting a deterministic policy from a pretrained DiffusionPlanner model and training with PDM-based safety scoring, our approach generates safe, comfortable trajectories while achieving real-time inference in complex traffic scenarios. Evaluation on nuPlan and interPlan benchmarks demonstrates that our method achieves the highest non-reactive nuPlan scores and aggregate interPlan scores among learning-based methods, while delivering an 8x speedup in inference time (12.41 ms versus 100.91 ms per trajectory) compared to the diffusion baseline. Our work provides a practical pathway for deploying efficient, safety-focused planning systems in real-world autonomous driving by leveraging pretrained diffusion models without requiring costly training from scratch, bridging the gap between diffusion model expressiveness and the latency requirements of production autonomous vehicles.

Supplementary Material

S1 Basics of Predictive Driver Model (PDM)

This Section complements Section 3.4 of the main paper. PDM [Dauner *et al.*, 2023; Yang *et al.*, 2024] evaluates trajectory safety and quality through a composite of weighted metrics. While the full PDM Scorer includes continuous metrics such as speed limit compliance and comfort, Figure S1 provides a supplementary overview of the primary spatial components used for trajectory selection. This includes monitoring the distance from the leading vehicle, divergence from the lane centerline, and adherence to the agent's reference path. A critical safety component is the maintenance of a Safe Distance from the leading vehicle, as shown in Figure S2. In the PDM framework, this is governed by high multiplier weights for Proximity and TTC (Time-to-Collision) within bounds, which penalize aggressive following behavior to minimize collision risk. As illustrated in Figure S3, Centerline Tracking is essential for maintaining Lane Following and Drivable Area Compliance. Precise centering ensures adequate clearance from neighboring vehicles, avoiding the penalties associated with drifting off-center. Finally, Figure S4 highlights Turning Behaviour, where Comfort metrics (weighted at 5 in PDM) penalize the aggressive lateral and longitudinal accelerations caused by late deceleration or overspeeding during maneuvers.

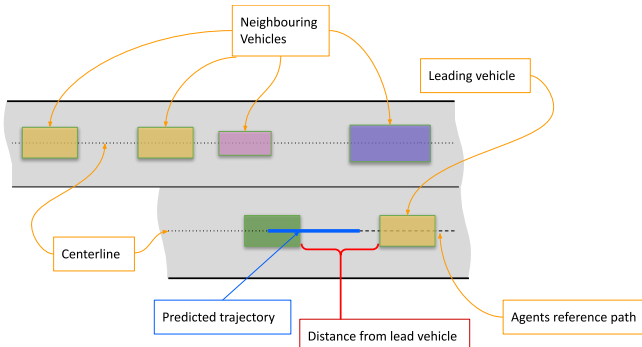


Figure S1: Supplementary overview of PDM metrics.

S2 Method Pseudocode

This Section complements Section 3.5 of the main paper. The complete algorithmic framework for the RAPiD pipeline is detailed in Algorithm 1 of this supplementary material. This pseudocode provides a formal technical roadmap for the three, *i.e.*, stage distillation process covering latent buffer creation, Implicit Q-Learning (IQL) critic training, and Score Regularised Policy Optimization (SRPO [Chen *et al.*, 2024]) policy extraction. By documenting the specific operations for

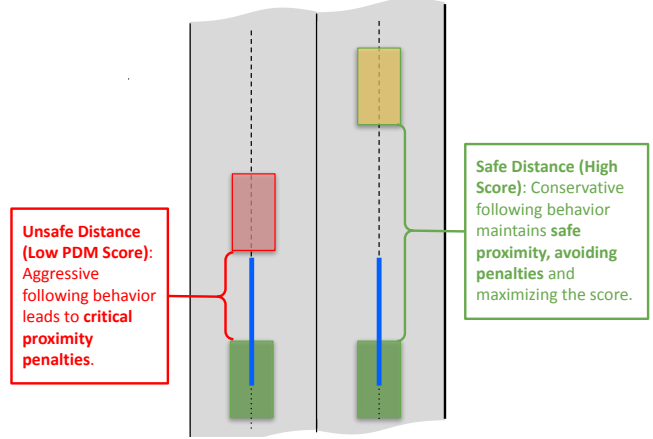


Figure S2: Visualisation of PDM safety distance metrics.

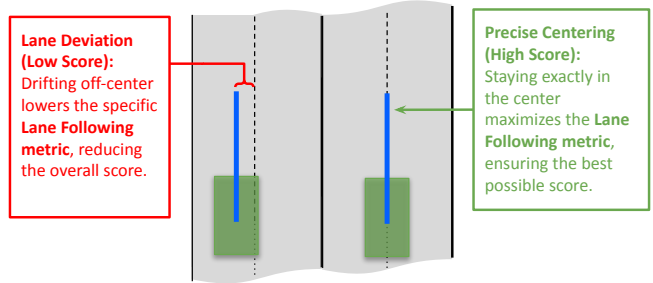


Figure S3: Analysis of Centerline tracking performance.

gradient updates and score regularization, this section ensures the reproducibility of our safety-focused deterministic policy.

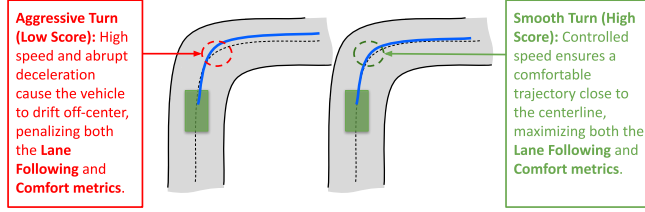


Figure S4: Qualitative evaluation of turning behavior.

Algorithm 1 RAPiD Training Pipeline

```

Require: Pretrained DiffusionPlanner Encoder  $\mathcal{E}$  and Denoiser  $\epsilon_\psi$  (Behavior Prior)
Require: PDM Scorer function  $\mathcal{S}_{\text{PDM}}$ 
Require: Ground truth dataset  $\mathcal{D}_{\text{raw}} = \{(s_{\text{raw}}, a_{\text{gt}})\}$ 
Require: Hyperparameters:  $\tau$  (expectile),  $\beta_{\text{AWR}}$ ,  $\lambda_\pi$ ,  $\beta$  (SRPO temp)

1: Stage 1: Offline Replay Buffer Creation
2: Initialize Replay Buffer  $\mathcal{D} \leftarrow \emptyset$ 
3: for each trajectory  $(s_{\text{raw}}, a_{\text{gt}}) \in \mathcal{D}_{\text{raw}}$  do
4:   Encode state:  $s \leftarrow \mathcal{E}(s_{\text{raw}})$  {Use pretrained encoder for latent dim}
5:   Compute Reward:  $r \leftarrow \mathcal{S}_{\text{PDM}}(s_{\text{raw}}, a_{\text{gt}})$  {Safety & Comfort metrics}
6:   Store transition:  $\mathcal{D} \leftarrow \mathcal{D} \cup \{(s, a_{\text{gt}}, r, s')\}$ 
7: end for
8: Stage 2: Critic Training (IQL) & Policy Pretraining
9: Initialize  $V_\zeta$ ,  $Q_\phi$ , and deterministic policy  $\pi_{\theta_{\text{init}}}$ 
10: while not converged do
11:   Sample batch  $B \sim \mathcal{D}$ 
12:   // Update Value Function (Expectile Regression)
13:    $\mathcal{L}_V(\zeta) \leftarrow \mathbb{E}_B [L_2^\tau(Q_\phi(s, a) - V_\zeta(s))]$ 
14:   Update  $\zeta \leftarrow \zeta - \alpha_V \nabla_\zeta \mathcal{L}_V$ 
15:   // Update Q-Function (TD Error)
16:    $y \leftarrow r + \gamma V_\zeta(s')$ 
17:    $\mathcal{L}_Q(\phi) \leftarrow \mathbb{E}_B [\|y - Q_\phi(s, a)\|_2^2]$ 
18:   Update  $\phi \leftarrow \phi - \alpha_Q \nabla_\phi \mathcal{L}_Q$ 
19:   // Pretrain Policy via Advantage Weighted Regression (AWR)
20:    $w \leftarrow \exp(\beta_{\text{AWR}}(Q_\phi(s, a) - V_\zeta(s)))$ 
21:    $\mathcal{L}_{\pi_{\text{init}}}(\theta_{\text{init}}) \leftarrow \mathbb{E}_B [w \cdot \|a - \pi_{\theta_{\text{init}}}(s)\|^2]$ 
22:   Update  $\theta_{\text{init}} \leftarrow \theta_{\text{init}} - \alpha_\pi \nabla_{\theta_{\text{init}}} \mathcal{L}_{\pi_{\text{init}}}$ 
23: end while
24: Stage 3: Policy Extraction via Score Regularization (SRPO)
25: Initialize  $\pi_\theta \leftarrow \pi_{\theta_{\text{init}}}$ 
26: while not converged do
27:   Sample batch  $s \sim \mathcal{D}$ 
28:    $a_\pi \leftarrow \pi_\theta(s)$ 
29:   // Compute Gradients for Q-maximization and Score Regularization
30:    $g_Q \leftarrow \nabla_a Q_\phi(s, a)|_{a=a_\pi}$ 
31:   Sample diffusion step  $t \sim U(0, T)$  and noise  $\epsilon \sim \mathcal{N}(0, I)$ 
32:    $a_t \leftarrow \alpha_t a_\pi + \sigma_t \epsilon$ 
33:    $g_{\text{score}} \leftarrow -\frac{1}{\beta} \omega(t)(\epsilon_\psi(a_t|s, t) - \epsilon)$ 
34:   // Surrogate Gradient Update
35:    $\nabla_\theta \mathcal{L}^{\text{surr}} \leftarrow (g_Q + g_{\text{score}}) \nabla_\theta \pi_\theta(s)$ 
36:   Update  $\theta \leftarrow \theta + \lambda_\pi \nabla_\theta \mathcal{L}^{\text{surr}}$ 
37: end while
38: return Trained Policy  $\pi_\theta$ 

```

S3 Additional Qualitative Analysis

This Section complements Section 4.2 of the main paper.

S3.1 Inference Timing and Decision-Making Comparison

A direct comparison of the planning timelines reveals that RAPiD initiates safety maneuvers much earlier than the teacher model. As shown in Figure S5b(b-1), RAPiD has already initiated a right-turn trajectory, demonstrating its ability to plan ahead for the maneuver. In contrast, DiffusionPlanner [Zheng *et al.*, 2025] in Figure S5a(a-1) shows no indication of planning for the turn. In Figure S5a(a-2), the teacher model finally initiates a right-turn decision. However, this is a delayed decision that occurs too late to safely account for the surrounding traffic. This latency leads to a catastrophic result as seen in Figure S5a(a-3), where the collision occurs because the vehicle followed a trajectory that should have been executed frames earlier. This difference in timing is driven by the PDM Scorer priorities used in our critic. By increasing the Comfort weight to 5 (from the nuPlan [Karnchanachari *et al.*, 2024] weight of 2) and applying a Proximity multiplier of 5, the policy becomes more sensitive to hazardous spatial relationships. While the teacher model focuses on Progress Along Route (nuPlan weight: 5), the distilled policy prioritizes safety and comfort, allowing it to act to successfully avert the collision.

S3.2 interPlan Scenario Based Analysis

We present detailed qualitative analysis of four challenging scenarios from the interPlan [Hallgarten *et al.*, 2023] benchmark. Figures S6-S9 show representative frames where DiffusionPlanner (frames a-d) and RAPiD (frames e-h) exhibit different planning behaviors. The predicted trajectories are shown as overlays on the scene images. These scenarios were selected to demonstrate critical safety differences in handling construction zones, jaywalking pedestrians, lane obstructions (nudge), and overtaking maneuvers.

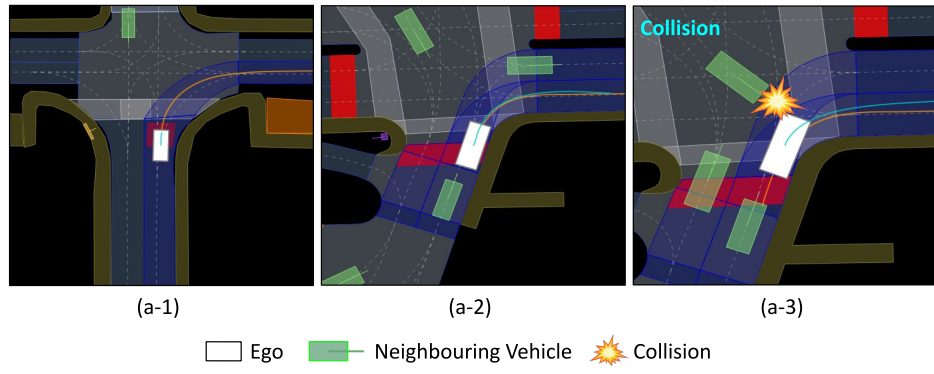
Construction Zone: In Figure S6(a), DiffusionPlanner begins moving away from the centerline toward the oncoming lane to navigate around the construction zone and workers. However, in Figure S6(b), we can see that despite this lateral movement, DiffusionPlanner does not maintain enough distance and comes dangerously close to the construction workers. In comparison, RAPiD begins its lateral maneuver earlier as shown in Figure S6(e), moving toward the oncoming lane while keeping a larger buffer from the construction zone. Figure S6(f) shows RAPiD successfully balancing between maintaining safe distance from the workers while not moving too far into the oncoming lane. Both planners return to the centerline after passing the construction zone, as seen in Figure S6(d) for DiffusionPlanner and Figure S6(h) for RAPiD.

Jaywalking: Figure S7(a) shows a pedestrian crossing the road mid-street (jaywalking), but DiffusionPlanner plans a trajectory that goes straight through where the pedestrian is standing. In Figure S7(b-c), we see that DiffusionPlanner does not adjust its plan in time and ends up colliding with the pedestrian. This represents a failure to prioritize safety over continuing along the route. In contrast, Figure S7(e)

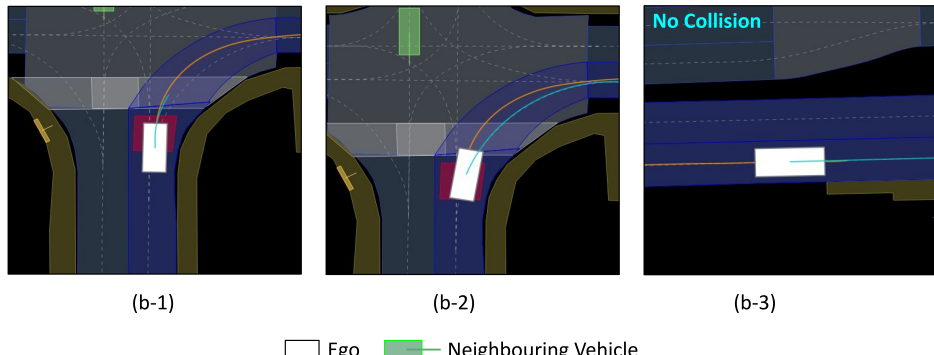
shows RAPiD planning to stop before reaching the pedestrian's position. Figure S7(f) shows RAPiD has come to a near-complete stop to avoid hitting the pedestrian. Once the pedestrian has moved out of the lane in Figure S7(g), RAPiD resumes driving in its intended direction as shown in Figure S7(h).

Nudge: In the nudge scenario, a vehicle is blocking part of the lane. Figure S8(a) shows DiffusionPlanner making a sharp lateral movement away from the blocked portion of the lane. However, Figure S8(b) reveals that this distance is still insufficient, resulting in a near-collision where the ego vehicle almost side-swipes the parked vehicle. RAPiD's approach in Figure S8(e) shows a smoother, more gradual lateral movement that begins earlier. Figure S8(f) demonstrates that RAPiD maintains a larger safety margin from the obstruction compared to DiffusionPlanner. This smoother trajectory planning allows RAPiD to avoid the near-collision situation entirely, as shown in Figure S8(g). Additionally, RAPiD returns to the lane center more smoothly in Figure S8(h), whereas DiffusionPlanner's return in Figure S8(d) appears more abrupt.

Overtake: In Figure S9(a), DiffusionPlanner detects a parked vehicle blocking part of its lane and begins moving into the oncoming lane to pass it. Figure S9(b) shows DiffusionPlanner successfully maintaining distance from the parked vehicle during the overtake. However, Figure S9(c-d) reveals a problem: DiffusionPlanner continues drifting into the oncoming lane even after passing the obstacle and fails to return to its own lane. This creates a dangerous situation with high risk of head-on collision. RAPiD's behavior in Figure S9(e) shows the beginning of its overtake maneuver, and Figure S9(f) demonstrates that RAPiD maintains a safe distance from the parked vehicle while minimizing how far it moves into the oncoming lane. Most importantly, Figure S9(g) shows that RAPiD has already returned to the center of its own lane immediately after passing the obstacle, completing the maneuver safely.



(a) **DiffusionPlanner**: Collision occurs at Frame 35 due to inference latency and lower proximity weighting.



(b) **RAPiD (Ours)**: Safe maneuver completed by Frame 20, enabled by deterministic low-latency and higher PDM safety weights.

Figure S5: Comparison of real-time decision making in a right-turn edge case from nuPlan’s “making right turn” scenario. The distilled policy (bottom) reacts 15 frames earlier than the DiffusionPlanner (top), successfully averting a collision.

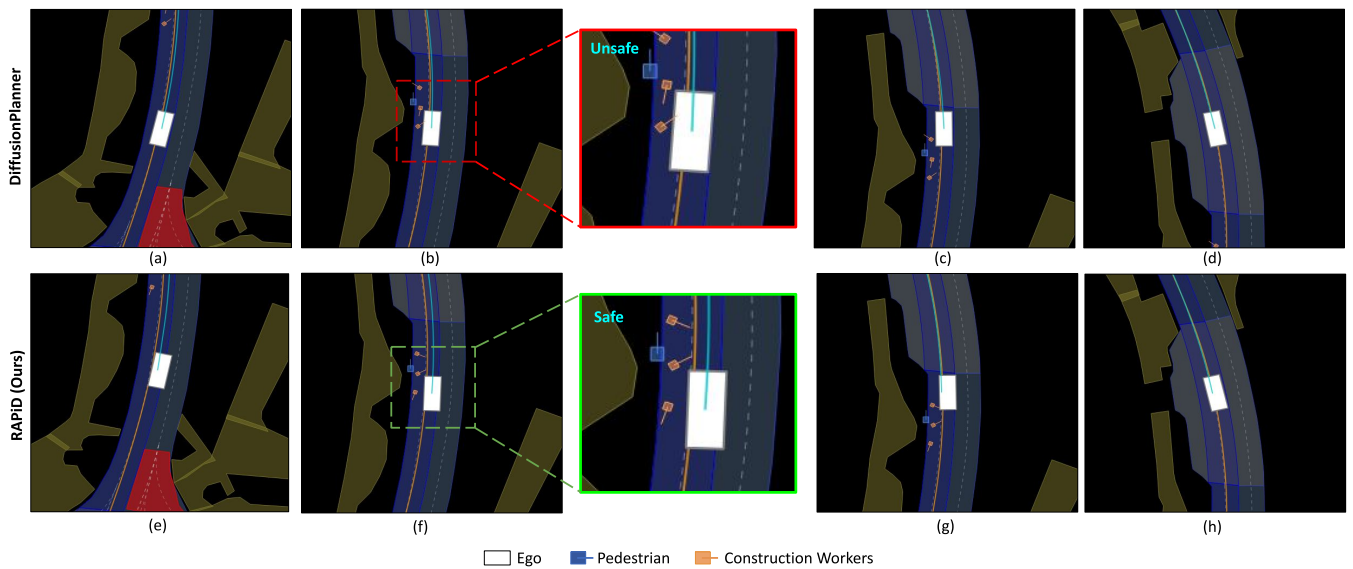


Figure S6: Construction zone scenario comparison between DiffusionPlanner (a-d) and RAPiD (e-h) in interPlan

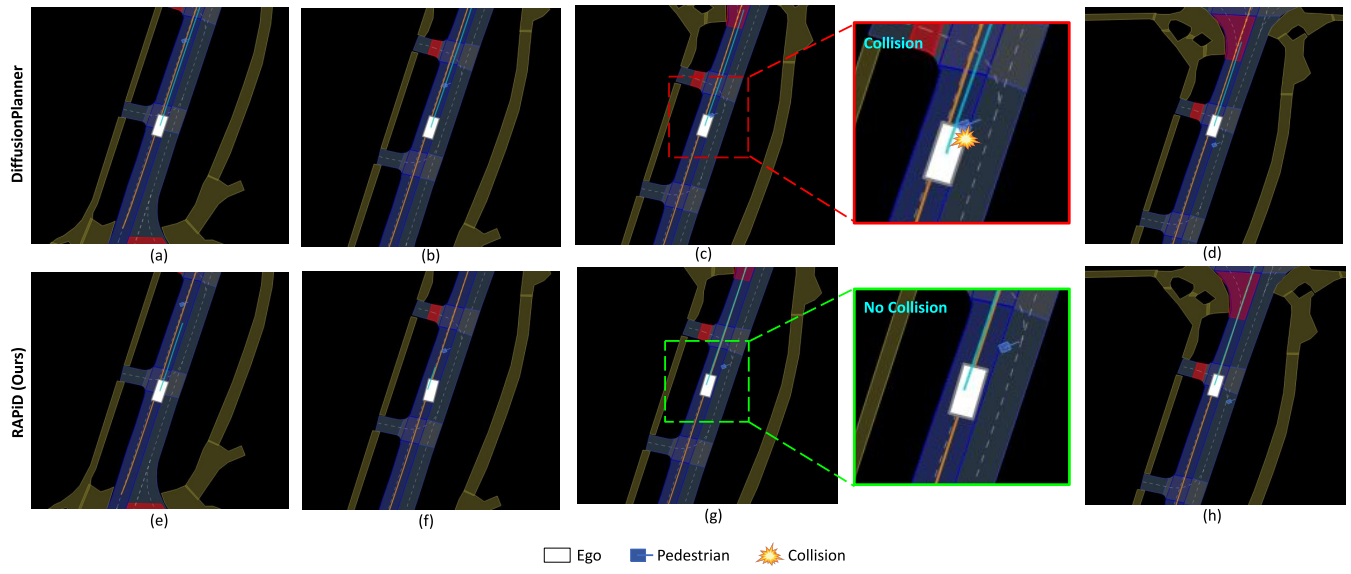


Figure S7: Jaywalking pedestrian scenario comparison between DiffusionPlanner (a-d) and RAPiD (e-h) in interPlan

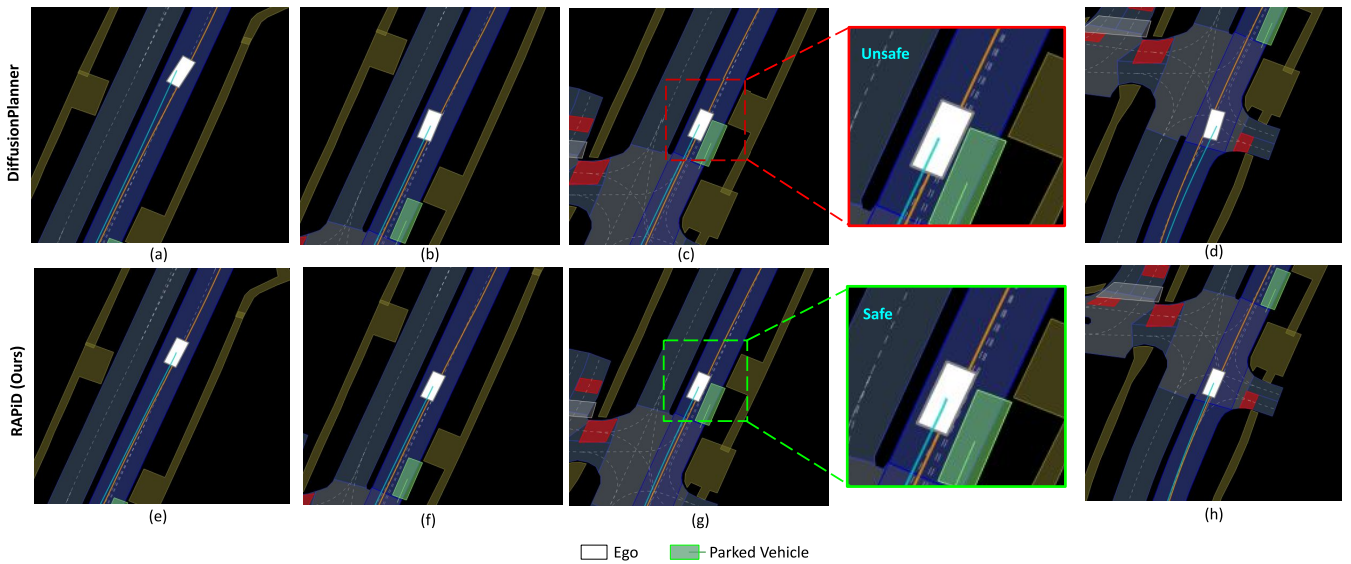


Figure S8: Nudge scenario with partial lane obstruction. DiffusionPlanner (a-d) vs RAPiD (e-h) in interPlan

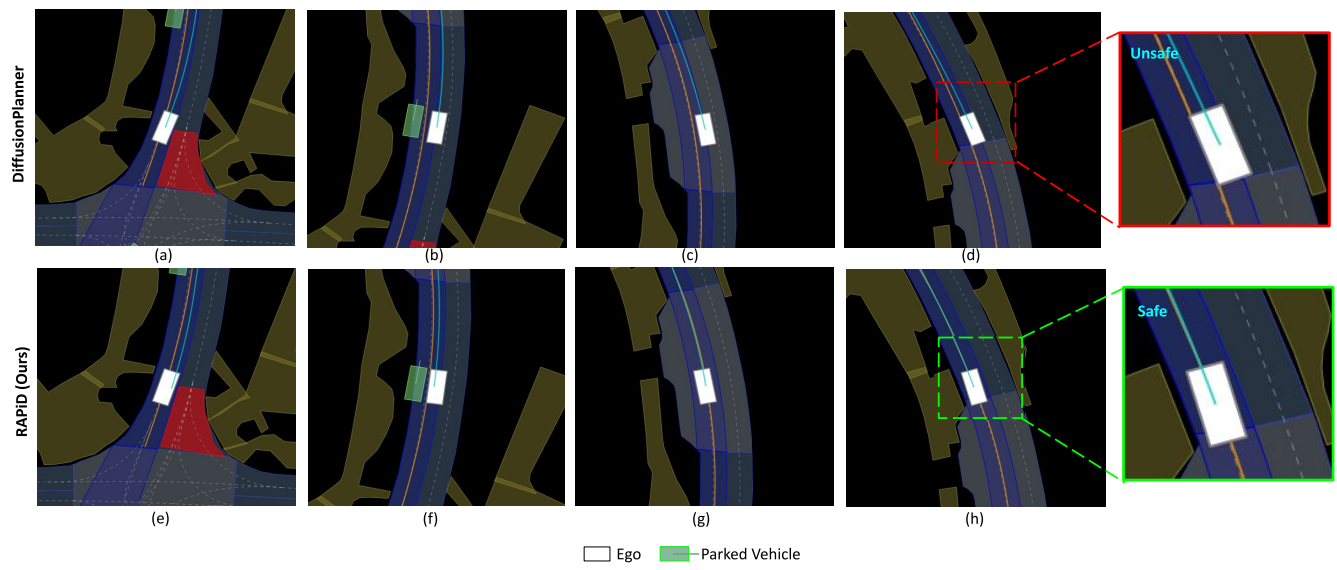


Figure S9: Overtake scenario with parked vehicle. DiffusionPlanner (a-d) vs RAPiD (e-h) in interPlan

References

[Ajay *et al.*, 2023] Anurag Ajay, Yilun Du, Abhi Gupta, Joshua B Tenenbaum, Tommi S Jaakkola, and Pulkit Agrawal. Is Conditional Generative Modeling all you need for Decision Making? In *The Eleventh International Conference on Learning Representations (ICLR)*, 2023.

[Bekey, 2005] George A. Bekey. *Autonomous Robots: From Biological Inspiration to Implementation and Control*. MIT Press, Cambridge, Massachusetts, 2005.

[Chen *et al.*, 2024] jie chang Chen, Cheng Lu, Zhengyi Wang, Hang Su, and Jun Zhu. Score Regularized Policy Optimization through Diffusion Behavior. In *The Twelfth International Conference on Learning Representations (ICLR)*, 2024.

[Cheng *et al.*, 2024] Jie Cheng, Yingbing Chen, and Qifeng Chen. Pluto: Pushing the limit of imitation learning-based planning for autonomous driving. *arXiv preprint arXiv:2404.14327*, 2024.

[Chi *et al.*, 2025] Cheng Chi, Zhenjia Xu, Siyuan Feng, Eric Cousineau, Yilun Du, Benjamin Burchfiel, Russ Tedrake, and Shuran Song. Diffusion policy: Visuomotor policy learning via action diffusion. *The International Journal of Robotics Research*, 44(10-11):1684–1704, 2025.

[Codevilla *et al.*, 2018] Felipe Codevilla, Matthias Müller, Antonio López, Vladlen Koltun, and Alexey Dosovitskiy. End-to-end Driving via Conditional Imitation Learning. In *2018 IEEE International Conference on Robotics and Automation (ICRA)*, pages 4693–4700. IEEE, 2018.

[Dauner *et al.*, 2023] Daniel Dauner, Marcel Hallgarten, Andreas Geiger, and Kashyap Chitta. Parting with Misconceptions about Learning-based vehicle motion planning. In *The 7th Conference on Robot Learning (CoRL 2023), Atlanta, USA*, pages 1268–1281. PMLR, 2023.

[Fujimoto *et al.*, 2019] Scott Fujimoto, David Meger, and Doina Precup. Off-policy deep reinforcement learning without exploration. In *The Proceedings of the 36th International Conference on Machine Learning (ICML)*, pages 2052–2062. PMLR, 2019.

[Hallgarten *et al.*, 2023] Marcel Hallgarten, Martin Stoll, and Andreas Zell. From prediction to planning with goal conditioned lane graph traversals. In *2023 IEEE 26th International Conference on Intelligent Transportation Systems (ITSC)*, pages 951–958. IEEE, 2023.

[Hallgarten *et al.*, 2024] Marcel Hallgarten, Julian Zapata, Martin Stoll, Katrin Renz, and Andreas Zell. Can vehicle motion planning generalize to realistic long-tail scenarios? In *2024 IEEE/RSJ International Conference on Intelligent Robots and Systems (IROS)*, pages 5388–5395. IEEE, 2024.

[Hansen-Estruch *et al.*, 2023] Philippe Hansen-Estruch, Ilya Kostrikov, Michael Janner, Jakub Grudzien Kuba, and Sergey Levine. IDQL: Implicit Q-learning as an actor-critic method with diffusion policies. *arXiv preprint arXiv:2304.10573*, 2023.

[Ho *et al.*, 2020] Jonathan Ho, Ajay Jain, and Pieter Abbeel. Denoising diffusion probabilistic models. *Advances in Neural Information Processing Systems 34: Annual Conference on Neural Information Processing Systems 2020 (NeurIPS)*, 33:6840–6851, 2020.

[Huang *et al.*, 2023] Zhiyu Huang, Haochen Liu, and Chen Lv. GameFormer: Game-theoretic modeling and learning of transformer-based interactive prediction and planning for autonomous driving. In *Proceedings of the IEEE/CVF International Conference on Computer Vision (ICCV)*, pages 3903–3913, 2023.

[Huang *et al.*, 2024] Zhiyu Huang, Peter Karkus, Boris Ivanovic, Yuxiao Chen, Marco Pavone, and Chen Lv. DTPP: Differentiable Joint Conditional Prediction and Cost Evaluation for Tree Policy Planning in Autonomous Driving. In *2024 IEEE International Conference on Robotics and Automation (ICRA)*, pages 6806–6812. IEEE, 2024.

[Karnchanachari *et al.*, 2024] Napat Karnchanachari, Dimitris Geromichalos, Kok Seang Tan, Nanxiang Li, Christopher Eriksen, Shakiba Yaghoubi, Noushin Mehdipour, Gianmarco Bernasconi, Whye Kit Fong, Yiluan Guo, et al. Towards learning-based planning: The nuplan benchmark for real-world autonomous driving. In *2024 IEEE International Conference on Robotics and Automation (ICRA)*, pages 629–636. IEEE, 2024.

[Kesting *et al.*, 2007] Arne Kesting, Martin Treiber, and Dirk Helbing. General lane-changing model MOBIL for car-following models. *Transportation Research Record*, 1999(1):86–94, 2007.

[Kostrikov *et al.*, 2021] Ilya Kostrikov, Ashvin Nair, and Sergey Levine. Offline Reinforcement Learning with Implicit Q-Learning. In *Deep RL Workshop NeurIPS 2021*, 2021.

[Kumar *et al.*, 2019] Aviral Kumar, Justin Fu, Matthew Soh, George Tucker, and Sergey Levine. Stabilizing off-policy q-learning via bootstrapping error reduction. *Advances in neural information processing systems: 33rd Conference on Neural Information Processing Systems (NeurIPS)*, 32, 2019.

[Peebles and Xie, 2023] William Peebles and Saining Xie. Scalable diffusion models with transformers. In *Proceedings of the IEEE/CVF International Conference on Computer Vision (ICCV)*, pages 4195–4205, 2023.

[Peng *et al.*, 2019] Xue Bin Peng, Aviral Kumar, Grace Zhang, and Sergey Levine. Advantage-weighted regression: Simple and scalable off-policy reinforcement learning. *arXiv preprint arXiv:1910.00177*, 2019.

[Rhinehart *et al.*, 2018] Nicholas Rhinehart, Rowan McAllister, and Sergey Levine. Deep imitative models for flexible inference, planning, and control. *arXiv preprint arXiv:1810.06544*, 2018.

[Scheel *et al.*, 2022] Oliver Scheel, Luca Bergamini, Maciej Wolczyk, Błażej Osiński, and Peter Ondruska. Urban driver: Learning to drive from real-world demonstrations

using policy gradients. In *Conference on Robot Learning (CoRL)*, pages 718–728. PMLR, 2022.

[Shafiuallah *et al.*, 2022] Nur Muhammad Mahi Shafiuallah, Zichen Jeff Cui, Ariuntuya Altanzaya, and Lerrel Pinto. Behavior Transformers: Cloning $\$k\$$ modes with one stone. In Alice H. Oh, Alekh Agarwal, Danielle Belgrave, and Kyunghyun Cho, editors, *Advances in Neural Information Processing Systems: 36th Conference on Neural Information Processing Systems (NeurIPS)*, 2022.

[Sohl-Dickstein *et al.*, 2015] Jascha Sohl-Dickstein, Eric Weiss, Niru Maheswaranathan, and Surya Ganguli. Deep unsupervised learning using nonequilibrium thermodynamics. In *International Conference on Machine Learning (ICML)*, pages 2256–2265. pmlr, 2015.

[Song *et al.*, 2021] Yang Song, Jascha Sohl-Dickstein, Diederik P Kingma, Abhishek Kumar, Stefano Ermon, and Ben Poole. Score-Based Generative Modeling through Stochastic Differential Equations. In *International Conference on Learning Representations (ICLR)*, 2021.

[Treiber *et al.*, 2000] Martin Treiber, Ansgar Hennecke, and Dirk Helbing. Congested traffic states in empirical observations and microscopic simulations. *Physical review E*, 62(2):1805, 2000.

[Wang *et al.*, 2023] Zhendong Wang, Jonathan J Hunt, and Mingyuan Zhou. Diffusion Policies as an Expressive Policy Class for Offline Reinforcement Learning. In *The Eleventh International Conference on Learning Representations (ICLR)*, 2023.

[Yang *et al.*, 2024] Brian Yang, Huangyuan Su, Nikolaos Gkanatsios, Tsung-Wei Ke, Ayush Jain, Jeff Schneider, and Katerina Fragkiadaki. Diffusion-Es: Gradient-Free Planning with Diffusion for Autonomous and Instruction-Guided Driving. In *2024 IEEE/CVF Conference on Computer Vision and Pattern Recognition (CVPR)*, pages 15342–15353, 2024.

[Zheng *et al.*, 2025] Yinan Zheng, Ruiming Liang, Kexin ZHENG, Jinliang Zheng, Liyuan Mao, Jianxiong Li, Weihao Gu, Rui Ai, Shengbo Eben Li, Xianyuan Zhan, et al. Diffusion-Based Planning for Autonomous Driving with Flexible Guidance. In *The Thirteenth International Conference on Learning Representations (ICLR)*, 2025.